Self-assembly of (A-comb-C)-b-(B-comb-C) diblock copolymer-based comb copolymers

Markov, V.; Subbotin, A.; ten Brinke, G.

Published in:
Physical Review E

DOI:
10.1103/PhysRevE.84.041807

Publication date:
2011

Self-assembly of (*A*-comb-*C*)-*b*-(*B*-comb-*C*) diblock copolymer-based comb copolymers

V. Markov,[1] A. Subbotin,[1,2] and G. ten Brinke[1,*]

[1]*Department of Polymer Chemistry and Zernike Institute for Advanced Materials, University of Groningen, Nijenborgh 4, NL-9747 AG Groningen, The Netherlands*

[2]*Institute of Petrochemical Synthesis, Russian Academy of Sciences, Moscow 119991, Russia*

(Received 11 May 2011; published 20 October 2011)

The phase behavior of (*A*-comb-*C*)-*b*-(*B*-comb-*C*) diblock copolymer melts is investigated using the strong segregation theory approach. Three different regimes are distinguished. In regime 1 both disordered comb blocks are microphase separated from each other, in regime 2 the side chains *C* are microphase separated from the disordered *A*-*b*-*B* diblock backbones, and, finally, in regime 3 all species *A*, *B*, and *C* are microphase separated. In the first regime the behavior is similar to that of a simple diblock copolymer melt with a renormalized Flory-Huggins interaction parameter. In regime 2 the region of stability of the different phases is significantly changed compared to simple diblocks due to the comb architecture. The fully microphase separated case, regime 3, is characterized by hierarchical structure formation. We restrict the analysis to systems where self-assembly results in the formation of alternating *C* layers and internally microphase separated *AB* layers. The latter consist of alternating *A* and *B* layers or disks of the minority component. In the former case, the *A* and *B* layers are generally perpendicular to the *C* layers. The parallel orientation is only possible for small grafting densities.

DOI: 10.1103/PhysRevE.84.041807 PACS number(s): 82.35.Jk

I. INTRODUCTION

The ability of block copolymer-based systems to form highly ordered complex nanostructures has been the focus of attention for many years [1–10]. This continued interest is driven by the prospects to develop nanotechnology applications such as nanostructured membranes, complex catalysts, nanowires, and photonic crystals, to mention only a few [11–14]. The self-assembly of diblock copolymers is well understood by now [5,6], although new developments still occur [7,8], and much of the research shifted to the study of self-assembly in copolymers with a more complex molecular architecture, such as tri-, star-, and multiblock copolymers, where already many new structures have been found experimentally and theoretically [15–24].

In the present paper we focus on comb copolymers, where the same types of side chains are attached to both blocks of a diblock copolymer. The structure formation in conventional comb copolymers, that is, with a homopolymer backbone, has already been presented in some detail in the literature [25–30]. Phase diagrams of various comb copolymer systems have been published and, although different in details, the general trends are the same as for diblock copolymers. Most importantly, rather than the overall chain length, it is the length of the "repeat unit" that determines the order-disorder transition temperature as well as the characteristic length scale of the ordered structures. Gido and co-workers [31–34] used this observation to initiate a strong segregation description of comb copolymers based on the so-called "constituting block copolymer hypothesis." According to this hypothesis, the repeat unit of a comb copolymer system is the determining factor for the microphase separated morphology. The weak segregation description of these systems lends further support to this proposition. The behavior of molecules with large, complex architectures is dictated by the behavior of the smaller architectural units from which they are comprised. Existing theory (e.g., Ref. [35]) is then used to predict the behavior of the repeat unit (i.e., the constituting block copolymer), which is then applied to the overall multigraft architecture.

Since the length scale of the structures corresponds to the length scale of the repeat unit, the characteristic domain size will usually be smaller than in the case of linear diblock copolymers. Combining a comb copolymer and a homopolymer into a comb-coil diblock copolymer molecule, the microphase separation between the homopolymer block and the comb block gives rise to a large length scale structure. Subsequent microphase separation inside the comb block containing domains will introduce the second shorter length scale [36,37]. The experimental realizations of these kinds of structures are all based on comb-coil diblock copolymer-based supramolecules, where the side chains of the comb block are bonded by physical interactions [38–42]. So far mainly diblock copolymers of polystyrene and poly(4-vinylpyridine), PS-*b*-P4VP, have been used in combination with, for example, pentadecylphenol (PDP) or dodecylbenzenesulfonic acid (DBSA), that form hydrogen bonds with the pyridine moiety of P4VP. Our current experimental activities seek to replace the PS block by another polymer block that also allows hydrogen bonding to PDP, thus obtaining supramolecular diblock copolymer-based comb copolymers [43]. In the present paper we present a theoretical strong segregation analysis of the self-assembly in such systems, assuming the side chains to be covalently linked to both blocks of the diblock copolymer backbone.

II. MODEL AND THEORETICAL APPROACH

A schematic representation of the (*A*-comb-*C*)-*b*-(*B*-comb-*C*) comb diblock-copolymer chains investigated is shown in Fig. 1. Before we start with the analysis we will introduce our notation.

*g.ten.brinke@rug.nl

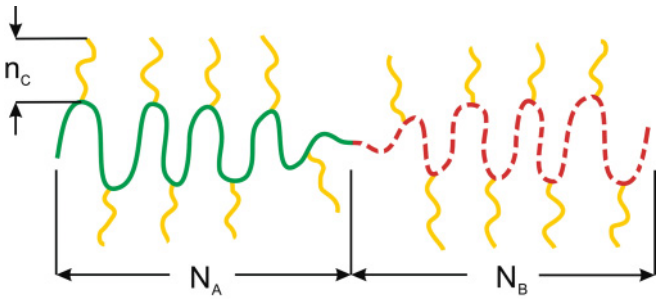

FIG. 1. (Color online) Schematic representation of comb-like diblock-copolymer chain.

The A and B blocks consist of N_A and N_B statistical segments, respectively. The C side chains contain n_C segments and the number of all C segments per copolymer chain is denoted by N_C. Hence the number m_C of C side chains per molecule is given by $m_C = N_C/n_C$. The total number of segments per copolymer chain is denoted by $2N$ and equals $N_A + \mathrm{N}_B + N_C = 2N$. It is assumed that all chain segments have the same length a and volume υ. The volume fraction of C segments is denoted by ϕ_C. The volume fractions of A and B blocks are $\phi_A = (1-\phi_C)\varphi_A$ and $\phi_B = (1-\phi_C)\varphi_B$, respectively, where φ_A (φ_B) denotes the volume fractions of the diblock backbone in absence of side chains, that is, $\varphi_B + \varphi_A = 1$. The length of the chain section between two neighboring C blocks is $n_b = (N_A + N_B)/m_C$, so that the A blocks contain $m_A = N_A/n_b$ short blocks of length n and the B blocks $m_B = N_B/n_b$ of such short blocks. Each of these short A and B blocks contains one C side chain grafted to the middle of it. The total number of $AC + BC$ repeat units in the copolymer chain is denoted as m ($m \equiv m_C$). Hence the total number of segments in the AC (BC) repeat unit equals $n = 2N/m$. Obviously, $m_A = \varphi_A m, m_B = \varphi_B m$, $n_b = n(1-\phi_C), n_C = n\phi_C$. We will assume that n is sufficiently larger than n_C so that the comb-copolymer chains do not form a bottle brush. The interactions between the segments of different types are described by the Flory-Huggins interaction parameters χ_{AB}, χ_{AC}, and χ_{BC}, all of which are assumed to be positive.

Our consideration will be based on the analysis of the free energy of the system which is written as

$$F = F_{\mathrm{conf}} + F_{\mathrm{int}}. \tag{2.1}$$

Here F_{int} is the interaction energy between the segments and F_{conf} is the conformational energy which in the strong segregation regime can be approximated as

$$F_{\mathrm{conf}} = F_{\mathrm{el}} + F_{\mathrm{grad}}, \tag{2.2}$$

where F_{el} is the stretching energy of the blocks and F_{grad} is the gradient term connected with nonhomogeneous profiles of the components. In our case the system after separation between different blocks has multidomain structure, at that thickness Δ of the interfacial layer between microphase separated domains is much smaller than the Gaussian size of the copolymer chain which is of the order of $R_0 = aN^{1/2}$. For such multidomain structure the free energy (2.1) after minimization with respect to the concentration profiles can be presented as

$$F = F_{\mathrm{el}} + F_{\mathrm{inf}} + F_{\mathrm{int}}, \tag{2.3}$$

where F_{inf} is the interfacial tension energy between domains and F_{int} is the interaction energy between segments in the domains. The minimization procedure for the different cases is given in the Appendix.

We first consider the disordered state which is realized when the values of the interaction parameters are sufficiently small. The dominating contribution to its free energy comes from the interactions between the different components, which per copolymer chain is given by

$$F_{\mathrm{DIS}} = 2N[\chi_{AB}(1-\phi_C)^2\varphi_A\varphi_B + \chi_{AC}\phi_C(1-\phi_C)\varphi_A + \chi_{BC}\phi_C(1-\phi_C)\varphi_B]. \tag{2.4}$$

We will consider it as the reference energy.

By increasing the unfavorable interactions between the segments various kinds of microphase separation between the different blocks become possible. We focus on three different situations, (1) microphase separation occurs between the AC and BC comb blocks only, (2) microphase separation occurs between the C blocks and the AB diblocks, and (3) microphase separation occurs between all block species A, B, and C. We will analyse these three situations employing the strong segregation limit (SSL). We will furthermore restrict our discussion to the simplest (classical) structures.

To denote the different self-assembled structures, superscripts will be used to indicate the different phases and subscripts to denote the minority phase. As an example, $HEX_{AC}^{AC/BC}$ denotes hexagonal microphase separation between the AC and BC comb blocks with the AC blocks forming the core of the cylinders.

III. *AC* COMB BLOCKS MICROPHASE SEPARATED FROM *BC* COMB BLOCKS

In the case of microphase separation between the AC and BC comb blocks only, the concentration profile of the C component is constant throughout the system, $\phi_C = \mathrm{const}$. The free energy can be presented in accordance with formula (2.3). The stretching energy F_{el} is calculated using Alexander–de Gene and Semenov approaches [2] for each type of structure. It is should be mentioned that F_{el} is the stretching energy of the A and B blocks only (it is assumed that C blocks are not stretched). The interfacial energy $\Delta F_{AC/BC}$ is derived in the Appendix, Eq. (A3).

A. Lamellar structure

When the volume fraction of the A and B components are sufficiently close to each other a lamellar structure will be formed. The layers consist of alternating AC and BC mixtures (Fig. 2). The A and B blocks are stretched in the direction perpendicular to the interface on a distance d_A and d_B, respectively. The C blocks are assumed not to be stretched.

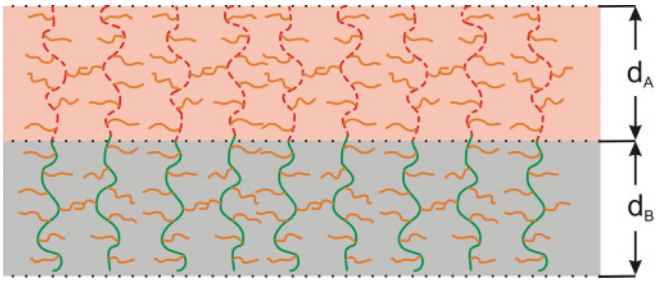

FIG. 2. (Color online) Schematic representation of the lamellar phase $LAM^{AC/BC}$ when AC blocks microphase separate from BC blocks.

We will use the Alexander–de Gennes approximation for the stretching energy of the A and B blocks, which implies that the free energy per copolymer chain is given by

$$F_{LAM^{AC/BC}} = \frac{3}{2}\frac{d_A^2}{N_A a^2} + \frac{3}{2}\frac{d_B^2}{N_B a^2} + \Sigma\gamma_{AC/BC} + F_{AC/BC}. \tag{3.1}$$

Here the first two terms represent the stretching energy of the A and B blocks, the third term is the interfacial free energy and the last term the interaction energy of the AC and BC mixtures. Minimization of this free energy with respect to the interfacial area Σ taking into account the incompressibility conditions

$$d_A\Sigma = 2N\varphi_A\upsilon, \quad d_B\Sigma = 2N\varphi_B\upsilon \tag{3.2}$$

results in the following period of the lamellar structure:

$$2(d_A + d_B) = \frac{4}{\sqrt{6}}R_0[\chi_{AB}N(1-\phi_C)^5]^{1/6}. \tag{3.3}$$

Its free energy is given by

$$F_{LAM^{AC/BC}} = 1.5(N\chi_{AB})^{1/3}(1-\phi_C)^{2/3} + 2N(1-\phi_C) \times \phi_C(\chi_{AC}\varphi_A + \chi_{BC}\varphi_B). \tag{3.4}$$

B. Hexagonal structure

When the volume fraction of B blocks (A blocks) decreases the formation of the hexagonal structure (Fig. 3) $HEX_{BC}^{AC/BC}$ ($HEX_{AC}^{AC/BC}$) is expected.

Assuming that the chains are stretched nonuniformly in the core [2] and uniformly in the shell, the free energy per copolymer chain in the hexagonal structure with the BC comb blocks forming the core can be written as

$$F_{HEX_{BC}^{AC/BC}} = \frac{R_{\rm in}^2}{N_B a^2}\left[\frac{\pi^2}{16} + \frac{3}{8}\ln\left(\frac{1}{\varphi_B}\right)\right] + 2\pi R_{\rm in}L\gamma_{AC/BC} + F_{AC/BC}, \tag{3.5}$$

where $\frac{R_{\rm in}^2}{N_B a^2}\frac{\pi^2}{16}$ is the stretching energy of the polymer chains forming the core and $\frac{R_{\rm in}^2}{N_B a^2}\frac{3}{8}\ln(\frac{1}{\varphi_B})$ is the stretching energy of the chains in the shell. The second term is the interfacial energy, with L the length of the cylinder per copolymer chain. After minimization of this energy with respect to $R_{\rm in}$ using the incompressibility conditions

$$\pi R_{\rm ex}^2 L = 2N\upsilon, \quad \pi R_{\rm in}^2 L = 2N\varphi_B\upsilon \tag{3.6}$$

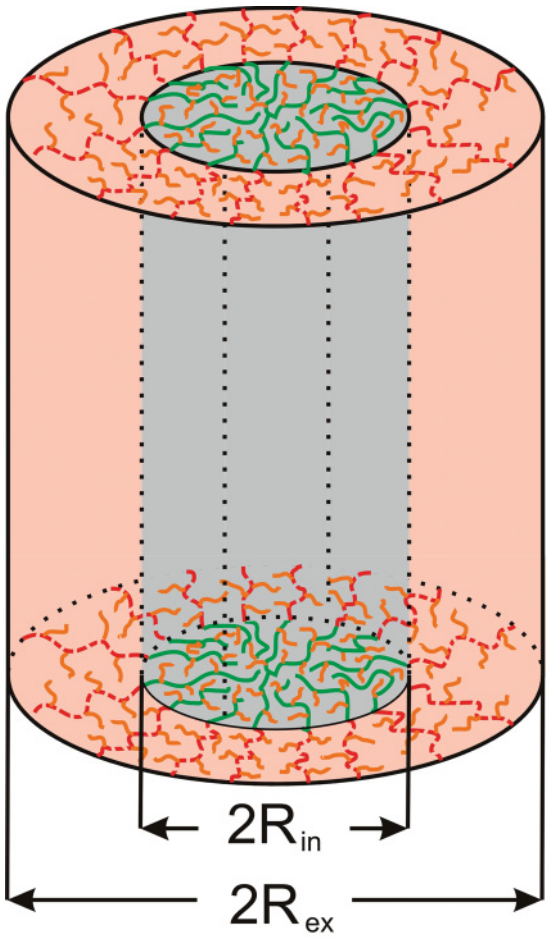

FIG. 3. (Color online) Schematic representation of the hexagonal phase $HEX_{BC}^{AC/BC}$, when the AC blocks microphase separate from the BC blocks that form the core.

we get

$$\mathrm{R_{in}} = 4R_0\left[\frac{\varphi_B^4(1-\phi_C)^5\chi_{AB}N}{6(\pi^2 - 6\ln\varphi_B)^2}\right]^{1/6}, \quad \mathrm{R_{ex}} = \mathrm{R_{in}}\varphi_B^{-1/2}. \tag{3.7}$$

The corresponding free energy per copolymer chain is

$$F_{HEX_{BC}^{AC/BC}} = 0.83(1-\phi_C)^{2/3}\varphi_B^{1/3}(\pi^2 - 6\ln\varphi_B)^{1/3}[N\chi_{AB}]^{1/3} + 2N(1-\phi_C)\phi_C(\chi_{AC}\varphi_A + \chi_{BC}\varphi_B). \tag{3.8}$$

Of course, when the AC comb blocks form the core a similar expression is obtained.

C. bcc structure

At a sufficiently small volume fraction of B blocks the $bcc_{BC}^{AC/BC}$ structure, with BC comb blocks forming the spheres, becomes preferable (Fig. 4). Using the same assumptions as for the hexagonal structure, the free energy per copolymer chain is given by

$$F_{bcc_{BC}^{AC/BC}} = \frac{R_{\rm in}^2}{N_B a^2}\left[\frac{3\pi^2}{80} + \frac{1}{2}\left(1-\varphi_B^{1/3}\right)\right] + \frac{1}{Q}4\pi R_{\rm in}^2\gamma_{AC/BC} + F_{AC/BC}, \tag{3.9}$$

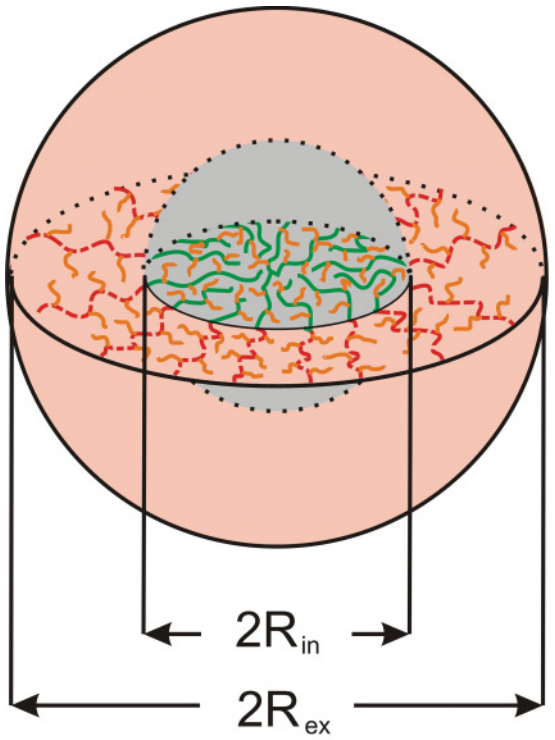

FIG. 4. (Color online) Schematic representation of $bcc_{BC}^{AC/BC}$ phase where the AC blocks microphase separate from the BC blocks that form the core.

where Q is the number of copolymer chains in the spherical domain. The stretching energy for the core is $\frac{R_{\rm in}^2}{N_B a^2}\frac{3\pi^2}{80}$, and for the shell $\frac{R_{\rm in}^2}{N_B a^2}\frac{1}{2}(1-\varphi_B^{1/3})$. The second term is the interfacial energy.

Incompressibility implies

$$\tfrac{4}{3}\pi R_{\rm ex}^3 = 2N\upsilon Q, \quad \tfrac{4}{3}\pi R_{\rm in}^3 = 2N\varphi_B\upsilon Q. \tag{3.10}$$

After minimization with respect to $R_{\rm in}$ the free energy is found to be

$$F_{bcc_{BC}^{AC/BC}} = 0.63(1-\phi_C)^{2/3}\varphi_B^{1/3}\left[3\pi^2+40\left(1-\varphi_B^{1/3}\right)\right]^{1/3} \times (N\chi_{AB})^{1/3}+2N(1-\phi_C)\phi_C(\chi_{AC}\varphi_A+\chi_{BC}\varphi_B). \tag{3.11}$$

The internal and external radii of the micelle are given by

$$\mathrm{R_{in}}=4R_0\left\{\frac{75\varphi_B^4(1-\phi_C)^5\chi_{AB}N}{8\left[3\pi^2+40\left(1-\varphi_B^{1/3}\right)\right]^2}\right\}^{1/6}, \quad \mathrm{R_{ex}}=\mathrm{R_{in}}\varphi_B^{-1/3}. \tag{3.12}$$

Again, the opposite case of AC comb blocks forming the core follows by a simple AB permutation.

Equations (2.4), (3.4), (3.8), and (3.11) allows us to construct phase diagrams for different volume fractions of the C component, where the transition from the disordered to the ordered state is estimated by comparing the free energy of the disordered state Eq. (2.4) with any of the SSL expressions (3.4), (3.8), and (3.11). Figure 5 shows the phase diagram in terms of $N\chi_{AB}$ versus the volume fraction φ_B of the B block in the A-b-B diblock for $\phi_C = 0.5, N\chi_{AC} = N\chi_{BC} = 10$

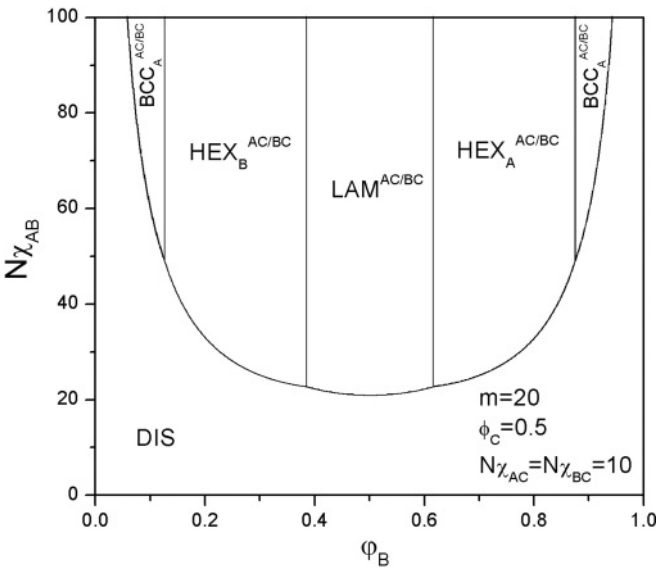

FIG. 5. Phase diagram for (A-comb-C)-b-(B-comb-C) when the C blocks are molecularly mixed with the microphase separated A and B blocks for fixed $m = 20, \phi_C = 0.5, N\chi_{AC} = N\chi_{BC} = 10$. Note, e.g., $HEX_{AC}^{AC/BC}$ denotes microphase separation between A-comb-C and B-comb-C with the former forming the core of the cylinders.

and total number of side chains $m = 20$. The critical Flory-Huggins parameter $\chi_{AB,c}$ corresponding to the order disorder transition at fixed $\varphi_B = 0.5$ is $2N\chi_{AB,c} \cong \frac{10.4}{(1-\varphi_C)^2}$. When the volume fraction of C blocks equals zero we arrive back at the simple diblock copolymer case of $2N\chi_{AB,c} \cong 10.4$. In the phase diagram (Fig. 5) the order-disorder transition occurs at $2N\chi_{AB,c} \cong 42$ for $\varphi_B = 0.5$.

IV. *AB* BACKBONE MICROPHASE SEPARATED FROM *C* SIDE CHAINS

Increasing the repulsion between the backbone and the side chains while at the same time reducing the repulsion between the A and B blocks results in the second type of microphase separation that we consider, that is, microphase separation between the side chains C on the one hand and the AB backbone on the other. As in the previous section the total free energy is defined by formula (2.3) where the stretching energy $F_{\rm el}$ is calculated for each structure individually and actually consists of known derivations for simple diblock [2]. Derivation of the interfacial energy $\Delta F_{AB/C}$ can be found in the Appendix, Eq. (A6).

A. Lamellar structure

Varying the volume fraction of the side chains and the value of the interaction parameters, different microphase separated morphologies can be formed. The simplest case corresponds to the lamellar structure where the alternating layers consist of C blocks and mixed A and B blocks. As shown in Fig. 6, the A and B chain sections between two successive C blocks can form either bridges or loops. To deal with this we will use the approximation that the stretching energies of loops and bridges are equal. A schematic picture of the lamellar structure with period $2(H_1 + H_2)$ is shown in Fig. 6.

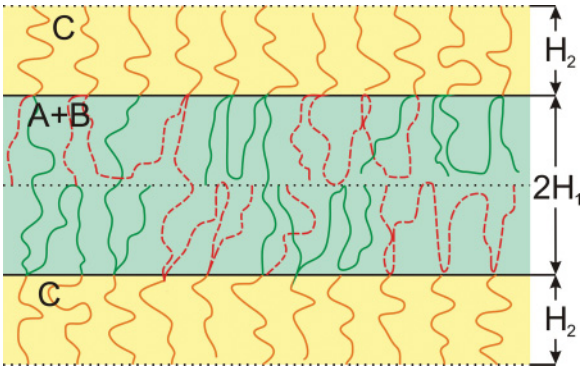

FIG. 6. (Color online) Lamellar structure $LAM^{AB/C}$ with C and AB lamellae.

The free energy of the lamellar structure per copolymer chain is given by

$$F_{LAM^{AB/C}} = m\frac{3H_2^2}{2n_C a^2} + m\frac{3(2H_1)^2}{2n_b a^2} + \Sigma\gamma_{AB/C} + \chi_{AB}\varphi_A\varphi_B(N_A + N_B). \quad (4.1)$$

Here the first term corresponds to stretching free energy of the C blocks, the second term represents the stretching free energy of the A and B blocks, the third term is the surface free energy of the $(AB)/C$ interface, and the last term is the interaction energy of the AB mixture.

Incompressibility implies

$$H_1\Sigma = 2N(1-\phi_C)\upsilon; \quad H_2\Sigma = 2N\phi_C\upsilon. \quad (4.2)$$

After minimization of the free energy with respect to Σ using Eq. (4.2) we obtain for the period of the structure

$$2(H_1+H_2) = \frac{4}{\sqrt{6}}R_0\left[\frac{N\chi_{AC}\varphi_A + N\chi_{BC}\varphi_B - N\chi_{AB}\varphi_A\varphi_B}{m^4(4-3\phi_C)^2}\right]^{1/6}. \quad (4.3)$$

Its free energy is

$$F_{LAM^{AB/C}} = 1.5m^{2/3}(4-3\phi_C)^{1/3}(N\chi_{AC}\varphi_A + N\chi_{BC}\varphi_B - N\chi_{AB}\varphi_A\varphi_B)^{1/3} + 2N\chi_{AB}\varphi_A\varphi_B(1-\phi_C). \quad (4.4)$$

For large values of N the free energy increases linearly with N.

B. Hexagonal structures

Besides the lamellar structure, two different hexagonally ordered cylindrical structures, denoted as $HEX_{AB}^{AB/C}$ and $HEX_{C}^{AB/C}$, are possible (Figs. 7 and 8). In the former the core of the cylinders is formed by the AB diblocks and in the latter by the C side chains. The internal and external radii of the cylinders are denoted as $R_{\rm in}$ and $R_{\rm ex}$, and L denotes the cylinder length per copolymer chain. When the core is formed by AB diblocks, the "short" A and B sections between consecutive side chains form only loops. The free energy of the $HEX_{AB}^{AB/C}$ phase can be written as:

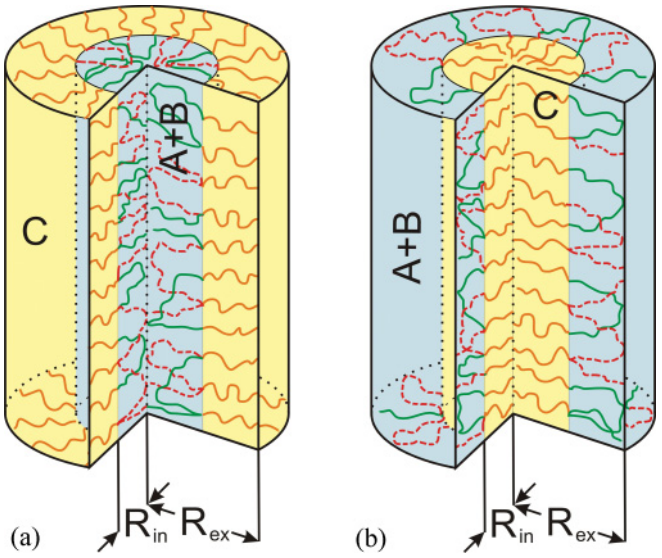

FIG. 7. (Color online) Schematic illustration of hexagonal structure: (a) $HEX_{AB}^{AB/C}$ with core of the cylinder formed by the AB diblocks and (b) $HEX_{C}^{AB/C}$ with core of the cylinder formed by the C side chains.

$$F_{HEX_{AB}^{AB/C}} = \frac{mR_{\rm in}^2}{a^2 n_b}\left[\frac{\pi^2}{4} + \frac{3}{8}\ln\left(\frac{1}{1-\phi_C}\right)\right] + 2\pi R_{\rm in}L\gamma_{AB/C} + \chi_{AB}\varphi_A\varphi_B(N_A+N_B). \quad (4.5)$$

Taking into account the incompressibility conditions $\pi R_{\rm ex}^2 L = 2N\upsilon$ and $\pi R_{\rm in}^2 L = 2N(1-\phi_C)\upsilon$, we obtain after

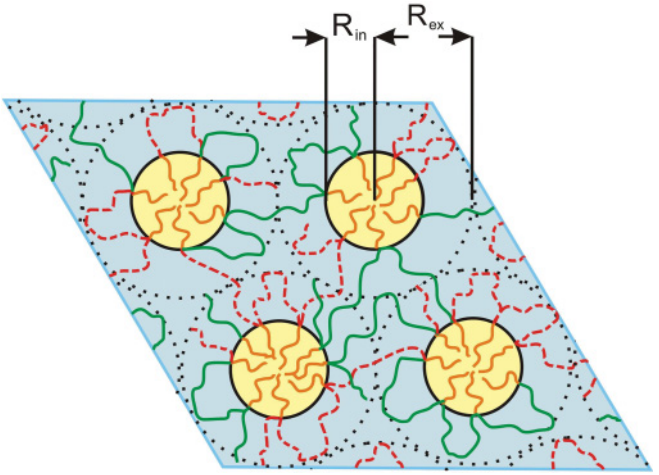

FIG. 8. (Color online) Schematic illustration of hexagonal structure $HEX_{C}^{AB/C}$, where the core of the cylinders is formed by the C side chains.

minimization of the free energy with respect to $R_{\rm in}$,

$$R_{\rm in} = R_0\left[\frac{4(1-\phi_C)^2}{\sqrt{6}\lambda_1 m^2}\right]^{\frac{1}{3}} \times (N\chi_{AC}\varphi_A + N\chi_{BC}\varphi_B - N\chi_{AB}\varphi_A\varphi_B)^{1/6},$$
$$R_{\rm ex} = R_{\rm in}(1-\varphi_C)^{-1/2}, \quad (4.6)$$

where $\lambda_1 = \frac{\pi^2}{4} + \frac{3}{8}\ln(\frac{1}{1-\phi_C})$. Using the expressions for $R_{\rm in}$ and $\gamma_{AB/C}$ the free energy can be written as

$$F_{HEX_{AB}^{AB/C}} = 2.08[\lambda_1 m^2(1-\phi_C)]^{1/3} \times (N\chi_{AC}\varphi_A + N\chi_{BC}\varphi_B - N\chi_{AB}\varphi_A\varphi_B)^{1/3} + 2N\chi_{AB}\varphi_A\varphi_B(1-\phi_C). \quad (4.7)$$

The other possibility arises when the volume fraction of the backbone is much higher than that of the side chains. In that case the AB diblocks form the matrix and, therefore, the copolymer chain can belong to more than one cylinder. Assuming again that the stretching free energy of the loops and the bridges connecting different elementary cells is equal, the free energy per copolymer chain is given by

$$F_{HEX_{C}^{AB/C}} = \frac{mR_{\rm in}^2}{n_C a^2}\left[\frac{\pi^2}{16} + \frac{3}{2}\ln\left(\frac{1}{\phi_C}\right)\right] + 2\pi R_{\rm in} L\gamma_{AB,C} + \chi_{AB}\varphi_A\varphi_B(N_A+N_B). \quad (4.8)$$

After minimization with respect to the radius of the core taking into account the incompressibility conditions $\pi R_{\rm ex}^2 L = 2N\upsilon$ and $\pi R_{\rm in}^2 L = 2N\phi_C\upsilon$ we get

$$R_{\rm in} = R_0\left(\frac{4\phi_C^2}{\sqrt{6}\lambda_2 m^2}\right)^{1/3} \times (N\chi_{AC}\varphi_A + N\chi_{BC}\varphi_B - N\chi_{AB}\varphi_A\varphi_B)^{1/6},$$
$$R_{\rm ex} = R_{\rm in}\varphi_C^{-1/2}, \quad (4.9)$$

where $\lambda_2 = \frac{\pi^2}{16} + \frac{3}{2}\ln(\frac{1}{\phi_C})$. Using this expression for $R_{\rm in}$ and the expression for $\gamma_{AB/C}$ the free energy becomes

$$F_{HEX_{C}^{AB/C}} = 2.08(\lambda_2 m^2\phi_C)^{1/3}(N\chi_{AC}\varphi_A + N\chi_{BC}\varphi_B - N\chi_{AB}\varphi_A\varphi_B)^{1/3} + 2N\chi_{AB}\varphi_A\varphi_B(1-\phi_C). \quad (4.10)$$

C. bcc structures

When the volume fraction of either C or AB is sufficiently small bcc structures may appear (see Fig. 9). Using the standard approach [2], the free energy of the $bcc_{AB}^{AB/C}$ structure when the core of the cylinders is formed by the AB diblocks is given by

$$F_{bcc_{AB}^{AB/C}} = \frac{mR_{\rm in}^2}{n_b a^2}\left\{\frac{3\pi^2}{20} + \frac{1}{2}[1-(1-\phi_C)^{1/3}]\right\} + \frac{4\pi}{Q}R_{\rm in}^2\gamma_{AB/C} + \chi_{AB}\varphi_A\varphi_B(N_A+N_B). \quad (4.11)$$

The incompressibility conditions are $\frac{4}{3}\pi R_{\rm ex}^2 = 2N\upsilon Q$ and $\frac{4}{3}\pi R_{\rm in}^2 = 2N(1-\phi_C)\upsilon Q$. When the matrix consists of the AB diblocks the free energy is given by

$$F_{bcc_{C}^{AB/C}} = \frac{mR_{\rm in}^2}{n_C a^2}\left\{\frac{3\pi^2}{80} + 2[1-(\phi_C)^{1/3}]\right\} + \frac{4\pi R_{\rm in}^2}{Q}\gamma_{AB/C} + \chi_{AB}\varphi_A\varphi_B(N_A+N_B). \quad (4.12)$$

The incompressibility conditions in this case read $\frac{4}{3}\pi R_{\rm ex}^2 = 2N\upsilon Q$ and $\frac{4}{3}\pi R_{\rm in}^2 = 2N\phi_C\upsilon Q$. After minimization of the corresponding free energies we arrive at the following results:

$$\mathrm{R}_{\mathrm{in},1} = R_0\left[\frac{\sqrt{6}(1-\phi_C)^2}{\mu_1 m^2}\right]^{1/3} \times (N\chi_{AC}\varphi_A + N\chi_{BC}\varphi_B - N\chi_{AB}\varphi_A\varphi_B)^{1/6},$$
$$\mathrm{R}_{\mathrm{ex},1} = \mathrm{R}_{\mathrm{in},1}(1-\phi_C)^{-1/3},$$
$$\mathrm{R}_{\mathrm{in},2} = R_{\rm in} = R_0\left(\frac{\sqrt{6}\phi_C^2}{\mu_2 m^2}\right)^{1/3} \times (N\chi_{AC}\varphi_A + N\chi_{BC}\varphi_B - N\chi_{AB}\varphi_A\varphi_B)^{1/6},$$
$$\mathrm{R}_{\mathrm{ex}} = \mathrm{R}_{\mathrm{in}}\phi_C^{-1/3}, \quad (4.13)$$

where

$$\mu_1 = \frac{3\pi^2}{20} + \frac{1}{2}[1-(1-\phi_C)^{1/3}], \quad \mu_2 = \frac{3\pi^2}{80} + 2\left(1-\phi_C^{1/3}\right).$$

Using Eqs. (4.11)–(4.13) the free energy of the $bcc_{AB}^{AB/C}$ phase (matrix of C blocks) can be written as

$$F_{bcc_{AB}^{AB/C}} = 2.72[\mu_1 m^2(1-\phi_C)]^{1/3}(N\chi_{AC}\varphi_A + N\chi_{BC}\varphi_B - N\chi_{AB}\varphi_A\varphi_B)^{1/3} + 2N\chi_{AB}\varphi_A\varphi_B(1-\phi_C). \quad (4.14)$$

For the second bcc phase (matrix of AB diblocks) we find

$$F_{bcc_{C}^{AB/C}} = 2.72(\mu_2 m^2\phi_C)^{1/3}(N\chi_{AC}\varphi_A + N\chi_{BC}\varphi_B - N\chi_{AB}\varphi_A\varphi_B)^{1/3} + 2N\chi_{AB}\varphi_A\varphi_B(1-\phi_C). \quad (4.15)$$

Free energies as a function of the volume fraction of C blocks for the different morphologies are shown in Fig. 10.

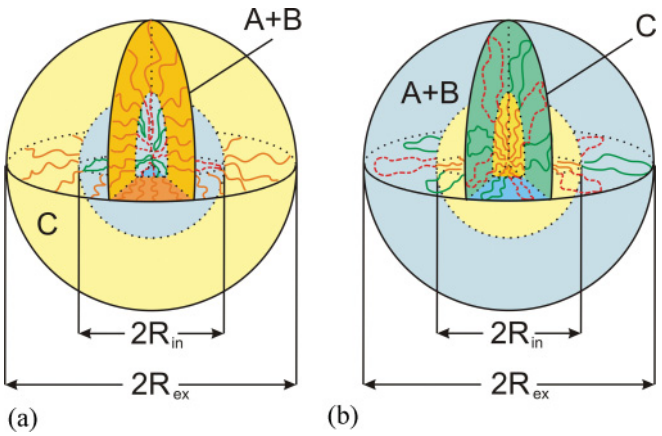

FIG. 9. (Color online) Schematic illustrations of the two bcc structures: (a) $bcc_{AB}^{AB/C}$, where core of the sphere is formed by AB diblocks and (b) $bcc_{C}^{AB/C}$, where core of the sphere is formed by the C side chains.

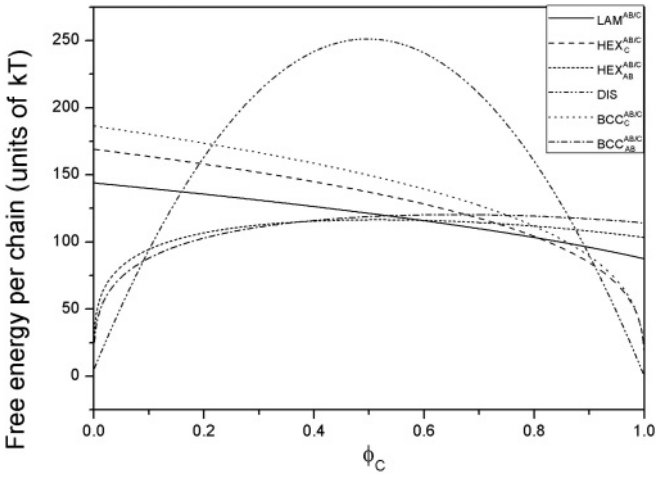

FIG. 10. Free energies as a function of the volume fraction ϕ_C of the C blocks for Flory-Huggins interaction parameters $\chi_{AB} = 0.01$, $\chi_{BC} = 0.5$, $\chi_{AC} = 0.5$, and $m = 20, N = 1000$. Here the notation of, e.g., HEX_C denotes hexagonal structure with C blocks forming the matrix.

It is easy to see that the free energy behavior of all the structures is asymmetric. This effect can be explained by the way the matrix is formed by either AB diblock chains or by C side chains. In Fig. 11 the stretching energy for the lamellar case of the AB diblocks and the C blocks versus the volume fraction of C blocks is presented at fixed values of the Flory-Huggins interaction parameters. It is easy to see that the stretching energy of the AB loops becomes equal to the stretching energy of C side chains when the volume fraction of the latter approximately equals $\phi_C = 0.8$. This big difference in stretching energies automatically leads to the asymmetric behavior observed.

Figure 12 presents one possible phase diagram in terms of the volume fraction of the C blocks and the interaction

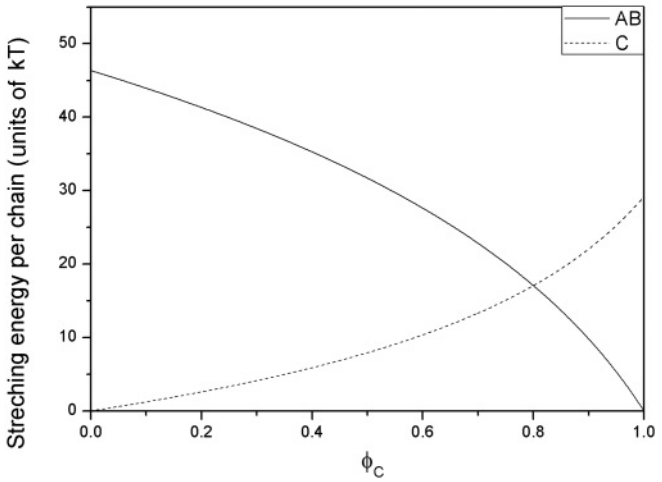

FIG. 11. Stretching energy for lamellar case for the AB diblocks and the C blocks vs the volume fraction ϕ_C of the C blocks for Flory-Huggins interaction parameters $\chi_{AB} = 0.01$, $\chi_{BC} = 0.5$, $\chi_{AC} = 0.5$, and $m = 20, N = 1000$. Solid line corresponds to stretching energy of AB blocks and dotted line to that of the C blocks.

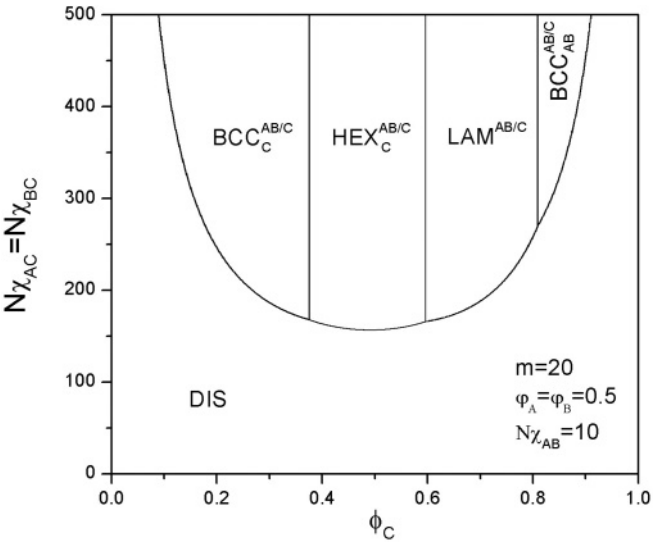

FIG. 12. Phase diagram of (A-comb-C)-b-(B-comb-C) when A and B are mixed as a function of the volume fraction ϕ_C of C blocks and interaction strength $N\chi_{AC} = N\chi_{BC}$ for fixed $N\chi_{AB} = 10$, $\varphi_A = \varphi_B = 0.5, m = 20$.

between C and AB diblocks, for fixed values $N\chi_{AB} = 10$, $m = 20$, $\phi_A = \phi_B = 0.5$.

The effect of the asymmetry is obvious. Compared to simple diblocks, the lamellar region shifts, in agreement with the analysis presented in Ref. [35], to higher values of the C volume fraction. At small values of the volume fraction of C blocks $\phi_C < 0.38$ the $bcc_C^{AB/C}$ structure with the cores formed by the C blocks becomes stable. At higher values of ϕ_C the hexagonal structure becomes preferable. For $0.6 < \phi_C < 0.8$ the lamellar structure is formed. A further increase of ϕ_C transfers the system directly into the $bcc_{AB}^{AB/C}$ phase where the core is formed by the AB blocks, thus bypassing the hexagonal structure. The hexagonal structure becomes unfavorable because of an insufficient amount of AB blocks to form the core.

V. HIERARCHICAL STRUCTURE FORMATION

Finally we consider the most interesting case where all three different types of blocks microphase separate from each other. For simplicity we restrict ourselves to the case where the C and $A + B$ monomers form a lamellar structure, with additional microphase separation between the A and B blocks inside the corresponding layer. Three different morphologies, namely a perpendicular lamellar-in-lamellar, a parallel lamellar-in-lamellar and a hexagonally packed disks-in-lamellar structure will be considered.

A. Perpendicular lamellar-in-lamellar structure

The perpendicular lamellar-in-lamellar structure can appear when the volume fraction of the B blocks is close to the volume fraction of the A blocks (Fig. 13). As above, we assume that the loops formed by the "short" A and B sections are stretched in the y direction (the direction perpendicular to the C layers) up to the mid plane (=distance H_1). In the x direction, which is perpendicular to the secondary lamellar

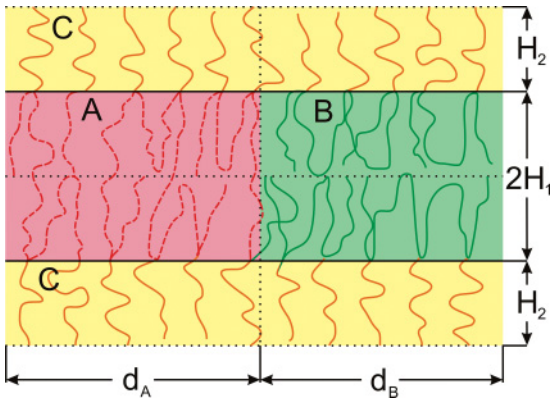

FIG. 13. (Color online) Schematic illustration of the perpendicular lamellar-*in*-lamellar structure.

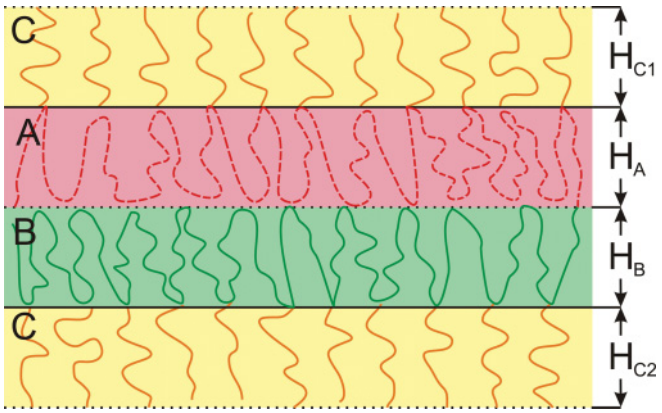

FIG. 14. (Color online) Schematic illustration of parallel lamellar-*in*-lamellar structure.

structure, the full A (B) blocks are stretched up to a distance d_A (d_B), respectively (see Fig. 13). The C blocks are stretched only in the y direction up to a distance H_2.

The free energy (per copolymer chain) of this structure can be approximated as the sum of the stretching and interfacial free energies:

$$F_{ll} = F_A + F_B + F_C + F_{AB} + F_{AC} + F_{BC}. \tag{5.1}$$

Here F_A, F_B, F_C are the stretching free energies of the A, B, and C blocks, respectively, given by

$$\begin{aligned} F_A &= F_{A,x} + F_{A,y} = \frac{3d_A^2}{2N_A a^2} + m_A \frac{3(2H_1)^2}{2n_b a^2}; \\ F_B &= F_{B,x} + F_{B,y} = \frac{3d_B^2}{2N_B a^2} + m_B \frac{3(2H_1)^2}{2n_b a^2} \\ F_C &= F_{C,y} = m_C \frac{3H_2^2}{2n_C a^2} \end{aligned} \tag{5.2}$$

and F_{AB}, F_{AC}, F_{BC} are the interfacial energies:

$$F_{AB} = \sum_{AB} \gamma_{AB}; \quad F_{AC} = \sum_{AC} \gamma_{AC}; \quad F_{BC} = \sum_{BC} \gamma_{BC}, \tag{5.3}$$

where $\sum_{AB}, \sum_{AC}, \sum_{BC}$ are the interfacial areas per copolymer chain. Incompressibility implies

$$\begin{aligned} \sum_{AC} H_1 &= \sum_{AB} d_A = N_A \upsilon; \\ \sum_{BC} H_1 &= \sum_{AB} d_B = N_B \upsilon; \\ \left(\sum_{AC} + \sum_{BC}\right) H_2 &= N_C \upsilon. \end{aligned} \tag{5.4}$$

After minimization of the free energy (5.1) with respect to the variables H_1, H_2, d_A, d_B, $\sum_{AC}, \sum_{BC}, \sum_{AB}$ using Eqs. (5.2)–(5.4) we find for the periods of the lamellar structure

$$\begin{aligned} 2(H_1 + H_2) &= 2\sqrt{\frac{2}{3}} R_0 \left[\frac{\varphi_B \sqrt{N\chi_{BC}} + (1-\varphi_B)\sqrt{N\chi_{AC}}}{m^2(4-3\phi_C)}\right]^{1/3}, \\ 2(d_A + d_B) &= 2\sqrt{\frac{2}{3}} R_0 (1-\phi_C)^{2/3} (N\chi_{AB})^{1/6}. \end{aligned} \tag{5.5}$$

Using these, the free energy (5.1) becomes

$$\begin{aligned} F_{\perp}^{A/B/C} = 1.5\{&(1-\phi_C)^{1/3}(N\chi_{AB})^{1/3} + m^{2/3}(4-3\phi_C)^{1/3} \\ &\times [(N\chi_{AC})^{1/2}(1-\varphi_B) + (N\chi_{BC})^{1/2}\varphi_B]^{2/3}\}. \end{aligned} \tag{5.6}$$

B. Parallel lamellar-*in*-lamellar structure

Another possibility is to have the AB interface parallel to the AC and BC interfaces as illustrated in Fig. 14. Now the stretching of the C blocks and the "short" A and B sections occurs only in the direction perpendicular to the interfaces between the components. The C blocks that are connected to the A blocks are stretched over a distance H_{C1} and the C blocks connected to the B blocks are stretched over a distance H_{C2}. The A blocks are stretched over a distance H_A and the B blocks over a distance H_B. Hence, the period of the lamellar structure is $H_{C1} + H_{C2} + H_A + H_B$.

The stretching free energies are given by

$$\begin{aligned} F_A &= 4m_A \frac{3H_A^2}{2n_b a^2}, \quad F_B = 4m_B \frac{3H_B^2}{2n_b a^2}, \\ F_C &= m_A \frac{3H_{C1}^2}{2n_C a^2} + m_B \frac{3H_{C2}^2}{2n_C a^2}. \end{aligned} \tag{5.7}$$

And the interfacial free energies by

$$F_{AB} = \Sigma\gamma_{AB}, \quad F_{AC} = \Sigma\gamma_{AC}, \quad F_{BC} = \Sigma\gamma_{BC}. \tag{5.8}$$

Incompressibility implies

$$\begin{aligned} 2N(1-\phi_C)\varphi_A \upsilon = \Sigma H_A, \quad 2N(1-\phi_C)\varphi_B \upsilon = \Sigma H_B, \\ 2N\phi_C\varphi_A \upsilon = \Sigma H_{C1}, \quad 2N\phi_C\varphi_B \upsilon = \Sigma H_{C2}. \end{aligned} \tag{5.9}$$

Here Σ is the interfacial area per copolymer chain (section) of the different components. After substitution of

Eqs. (5.7)–(5.8) in the free energy Eq. (5.1) and minimization the period is found to be

$$H_{C1}+H_{C2}+H_A+H_B = \sqrt{\frac{2}{3}}R_0\left[\frac{(\sqrt{N\chi_{AC}}+\sqrt{N\chi_{BC}}+\sqrt{N\chi_{AB}})}{m^2\big((1-\varphi_B)^3+\varphi_B^3\big)(4-3\phi_C)}\right]^{1/3}. \tag{5.10}$$

With this the free energy becomes

$$F_{||}^{A/B/C} = 1.5m^{2/3}\big[\varphi_B^3+(1-\varphi_B)^3\big]^{1/3}(4-3\phi_C)^{1/3} \times(\sqrt{N\chi_{AC}}+\sqrt{N\chi_{BC}}+\sqrt{N\chi_{AB}})^{2/3}. \tag{5.11}$$

The free energy of the parallel lamellar-*in*-lamellar structure is a function of $[\varphi_B^3+(1-\varphi_B)^3]^{1/3}$ with a minimum at $\varphi_B=0.5$.

C. Hexagonally packed disks in lamellar structure

When the volume fraction of the B or A component is sufficiently small, microphase separation inside the AB layers may result in hexagonally packed disks with the core of the disks formed by the minority component (Fig. 15). Suppose the B blocks form the core and the A blocks the matrix. The C blocks form lamellar layers. The thickness of the C layers is $2H_2$ and the thickness of the AB layers is $2H_1$.

As always, the free energy of the structure can be written as the sum of the elastic and the interfacial free energies (5.1). The stretching free energies of the different blocks are given by

$$F_A = F_{A,x}+F_{A,y} = \frac{3}{8}\frac{R_{\rm in}^2}{N_Aa^2}\ln\frac{1}{\varphi_A}+m_A\frac{3(2H_1)^2}{2n_ba^2},$$
$$F_B = F_{B,x}+F_{B,y} = \frac{\pi^2}{16}\frac{R_{\rm in}^2}{N_Aa^2}+m_B\frac{3(2H_1)^2}{2n_ba^2}, \tag{5.12}$$
$$F_C = F_{C,y} = m_C\frac{3H_2^2}{2n_Ca^2}.$$

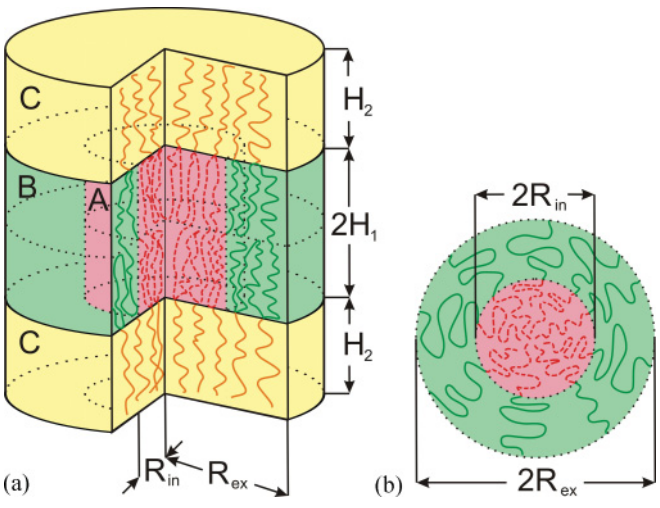

FIG. 15. (Color online) Schematic illustrations of hexagonally packed disks inside a lamellar structure: (a) three dimensional view and (b) interface between AB and C blocks.

The interfacial energies F_{AB},F_{AC},F_{BC} are

$$F_{AB}=4\pi R_{\rm in}H_1\gamma_{AB}Q^{-1},\quad F_{BC}=2\pi\big(R_{\rm ex}^2-R_{\rm in}^2\big)\gamma_{BC}Q^{-1},$$
$$F_{AC}=2\pi R_{\rm in}^2\gamma_{AC}Q^{-1}, \tag{5.13}$$

where Q is the number of copolymer chains per disk.

Incompressibility implies

$$2\pi R_{\rm ex}^2H_1=(N_A+N_B)\upsilon Q,\quad 2\pi R_{\rm in}^2H_1=N_A\upsilon Q,$$
$$2\pi R_{\rm ex}^2H_2=N_C\upsilon Q. \tag{5.14}$$

When $Q\gg1$ (this condition will be verified afterwards) minimization of the total free energy (5.1) with respect to parameters of the hexagonal structure using Eqs. (5.12)–(5.14) results in a period $2(H_1+H_2)$ and a radius $R_{\rm in}$ given by

$$2(H_1+H_2)=2\sqrt{\frac{2}{3}}R_0\left[\frac{\varphi_A\sqrt{N\chi_{BC}}+(1-\varphi_A)\sqrt{N\chi_{AC}}}{m^2(4-3\phi_C)}\right]^{1/3},$$

$$R_{\rm in}=R_0\left[\frac{4\varphi_A^2(1-\phi_C)^2}{\sqrt{6}\big(\frac{\pi^2}{16}-\frac{3}{8}\ln\varphi\big)}\right]^{1/3}(N\chi_{AB})^{1/6}. \tag{5.15}$$

This results in a free energy given by

$$F_{HEX_B^{A/B/C}} = 1.5m^{2/3}(4-3\phi_C)^{1/3}[(1-\varphi_A)\sqrt{N\chi_{AC}} +\varphi_A\sqrt{N\chi_{BC}}]^{2/3}+2.08\varphi_A^{2/3}(1-\phi_C)^{1/3} \times\left(\frac{\pi^2}{16}-\frac{3}{8}\ln\varphi_A\right)^{1/3}(N\chi_{AB})^{1/2}. \tag{5.16}$$

The number of chains per disk is found to satisfy

$$Q=7.2\pi N^{1/2} \times\frac{\varphi_A^{1/3}[\varphi_A\sqrt{N\chi_{BC}}+(1-\varphi_A)\sqrt{N\chi_{AC}}]^{1/3}(N\chi_{AB})^{1/3}}{m^{2/3}(\pi^2-6\ln\varphi_A)^{2/3}} \times\frac{(1-\phi_C)^{4/3}}{(4-3\phi_C)^{1/3}}. \tag{5.17}$$

In order to prove the assertion that $Q\gg1$, Q is plotted in Figs. 16 and 17 as a function of the composition (interaction) parameters. Figure 16 demonstrates that for $\varphi_A>0.1$ and $\phi_C<0.95$ the number of chains $Q>10$ for interaction parameter values satisfying $N\chi_{AB}=100, N\chi_{AC}=N\chi_{BC}=200$.

Figure 17 shows Q as a function of the interaction parameters $N\chi_{AB},N\chi_{AC},N\chi_{BC}$ at fixed volume densities when the hexagonal structure is formed. Starting from $N\chi=50$ the number of chains remains at $Q>10$.

VI. PHASE DIAGRAMS

We will now discuss several scenarios. We start with fixed volume fractions $\phi_C=0.7,\varphi_A=\varphi_B=0.5$ and plot phase diagrams in the $(N\chi_{AB},N\chi_{AC}=N\chi_{BC})$ plane for different values of the number of side chains m. Because of the volume fractions selected only lamellar domains are possible (cf. Fig. 12). At sufficiently small values of the Flory-Huggins interaction parameters $\chi_{AB},\chi_{AC},\chi_{BC}$ the disordered state DIS is stable. By increasing the interaction between the A and B blocks, keeping the interaction between backbone and side

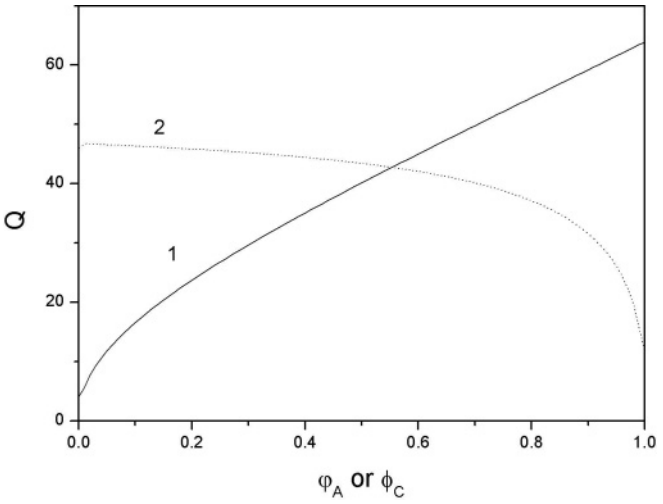

FIG. 16. The number of chains Q per disk as a function of different volume factions: (1) φ_A at fixed $\phi_C = 0.7$ and (2) ϕ_C at fixed $\varphi_A = 0.5$. All calculations were performed at fixed $N\chi_{AB} = 100, N\chi_{AC} = N\chi_{BC} = 200$.

chains fixed, the system self-assembles in the lamellar state $LAM^{AC/BC}$ with alternating layers formed by AC and BC mixtures. As discussed above, this regime corresponds to that of simple symmetric diblocks with effective Flory-Huggins parameter $(1-\phi_C)^2\chi_{AB}$. On the other hand, if the interaction between the A and B blocks remains sufficiently small and the interaction between the backbone and the side chains increases, at some point a lamellar state $LAM^{AB/C}$ will be formed with alternating layers consisting of C side chains and AB mixtures. At sufficiently high values of all three interaction parameters all three components will microphase separate from each other. Then two types of lamellar phases are possible, one where the layers formed by the A or B blocks are aligned perpendicularly with respect to layers formed by the C blocks, $LAM_{\perp}^{A/B/C}$, and one where all layers are parallel,

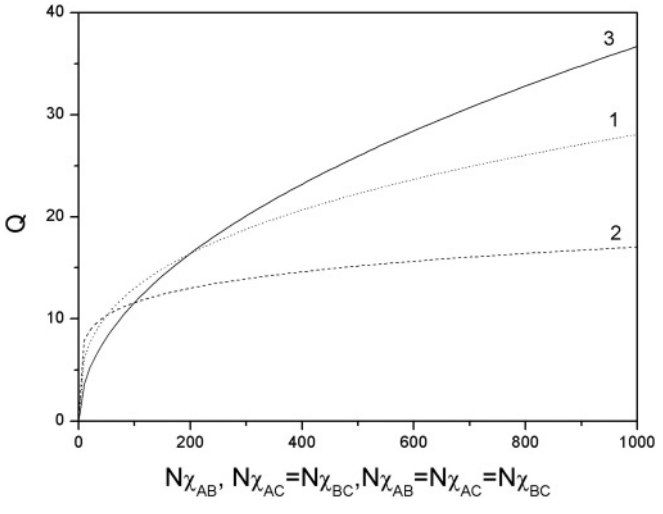

FIG. 17. The number of chains Q per disk as a function of the Flory-Huggins interaction parameters: (1) $N\chi_{AB}$, (2) $N\chi_{AC} = N\chi_{BC}$, and (3) $N\chi_{AB} = N\chi_{AC} = N\chi_{BC}$ at fixed $\varphi_A = 0.1, \phi_C = 0.9$. Extreme values were chosen to prove that Q does not drop below 10.

$LAM_{||}^{A/B/C}$. Figure 18(a) presents the phase diagram for $m = 2$. The transition between the partially and fully microphase separated states occurs at small values of $N\chi_{AB}$ (from $LAM^{AC/BC}$ to $LAM_{\perp}^{A/B/C}$) and small values of $N\chi_{AC} = N\chi_{BC}$ (from $LAM^{AB/C}$ to $LAM_{||}^{A/B/C}$). The border between parallel lamellar-in-lamellar and perpendicular lamellar-in-lamellar is the straight line $N\chi_{AB} = 2N\chi_{AC} = 2N\chi_{BC}$. At $m = 3$ [Fig. 18(b)] the region of parallel lamellar-in-lamellar $LAM_{||}^{A/B/C}$ becomes smaller and the straight transition line between $LAM_{||}^{A/B/C}$ and $LAM_{\perp}^{A/B/C}$ changes into $N\chi_{AB} = 0.28N\chi_{AC} = 0.28N\chi_{BC}$. At higher values of m the parallel lamellar-in-lamellar phase disappears [Fig. 18(c)]. Increasing the number of side chains m the chain sections between consecutive side chains and the side chains become shorter and higher values of the Flory-Huggins parameters are required to induce microphase separation. As a consequence, the stability regions of $LAM^{AB/C}$, $LAM^{AC/BC}$, and the disordered phase DIS all increase. The parallel lamellar-in-lamellar phase becomes unfavorable due to the high AB interfacial energy. In Fig. 19 the free energies of the parallel and perpendicular lamellar phases are shown as a function of the number of side chains m. For the fixed values of the other parameters selected, the free energies become approximately the same for $m = 3$.

Next we turn our attention to asymmetric diblock backbones. Figure 20 presents phase diagrams as a function of the Flory-Huggins interaction parameters $N\chi_{AC} = N\chi_{BC}$ and the volume fraction φ_B of B. The diagrams are calculated at a fixed volume fraction of C blocks $\phi_C = 0.7$, because in that case the fully separated system consists of alternating C and AB layers with different internal structures in the AB layers. Figure 20(a) corresponds to $m = 10, N\chi_{AB} = 200$. In this case, as long as $N\chi_{AC} = N\chi_{BC} < 100$, the phase behavior has already been presented in phase diagram Fig. 5. When $N\chi_{AC} = N\chi_{BC} > 100$, four different phases are stable. As a function of the volume fraction φ_B these are the lamellar $LAM^{AB/C}$ phase, the disk-in-lamellar phase $HEX_B^{A/B/C}$ (Fig. 15, core formed by B), the perpendicular lamellar-in-lamellar structure $LAM_{\perp}^{A/B/C}$, and the disk-in-lamellar phase $HEX_A^{A/B/C}$ (core formed by A) and again the lamellar $LAM^{AB/C}$ phase. For sufficiently low or high volume fraction φ_B the A and B blocks form a disordered phase and the system essentially resembles a simple comb copolymer system. When $m = 2$ [Fig. 20(b)] the parallel lamellar-in-lamellar state $LAM_{||}^{A/B/C}$ appears in the range $0.385 < \varphi_B < 0.615$. At $\varphi_B = 0.5$ the lowest transition point occurs at $N\chi_{AC}{=}N\chi_{BC} \approx 98$. The border line between the fully microphase separated system and AC/BC phases shifts to smaller values of Flory-Huggins interaction parameters $N\chi_{AC} = N\chi_{BC} \approx 25$.

Decreasing $N\chi_{AB}$ to 100 changes the phase diagram considerably [Fig. 20(c)]. The bcc phases are not stable anymore and the width of disordered state area increases.

Figure 21 presents another series of phase diagrams, now in terms of the Flory-Huggins interaction parameters $N\chi_{AB}$ and the volume fraction of B blocks φ_B. For fixed values $m = 20, N\chi_{AC} = N\chi_{BC} = 200, \phi_C = 0.7$ four different structures are possible. At small values of $N\chi_{AB} < 24$ the lamellar phase with mixed AB blocks $LAM^{AB/C}$ is formed. The borders between the different structures are similar to the borders in the phase diagram for simple diblock copolymers with the

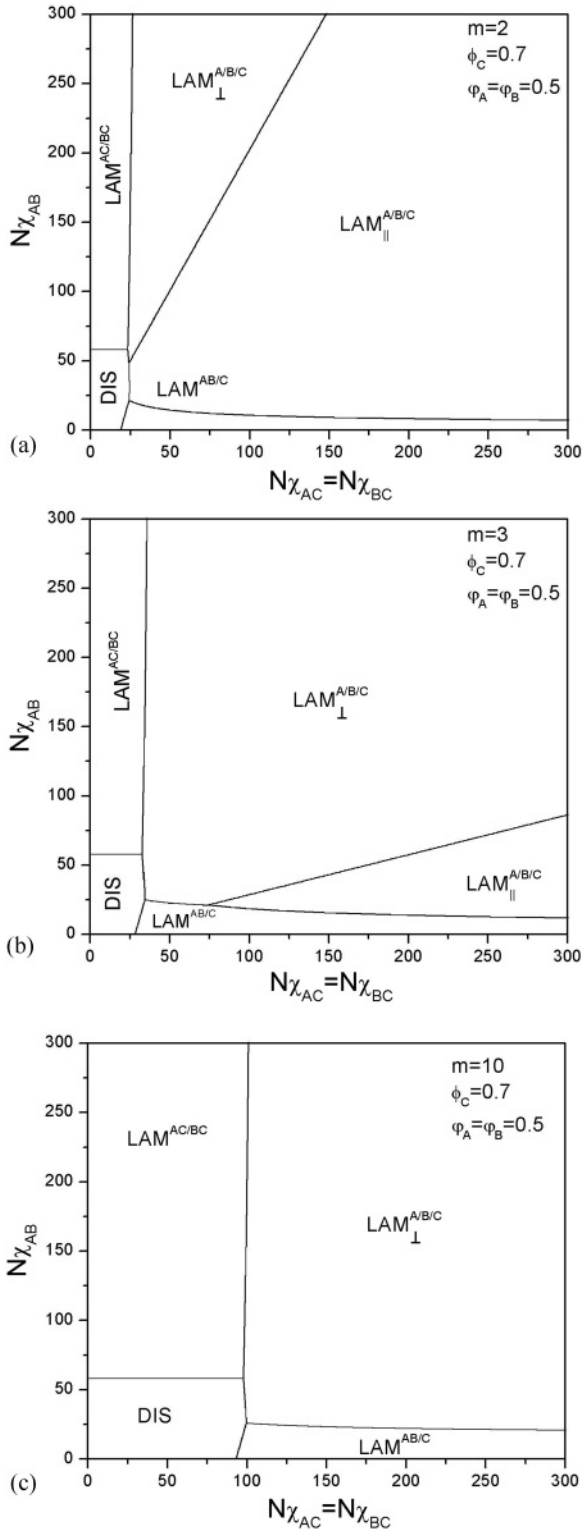

FIG. 18. Phase diagrams of the lamellar phases of (*A*-comb-*C*)-*b*-(*B*-comb-*C*) as a function of the Flory-Huggins interaction parameters $N\chi_{AB}$ and $N\chi_{AC} = N\chi_{BC}$ for fixed $\phi_C = 0.7, \varphi_A = \varphi_B = 0.5$: (a) $m = 2$; (b) $m = 3$; and (c) $m = 10$.

noticeable exception that the bcc structure is absent. Of course, the disordered state of the latter is replaced by the $LAM^{AB/C}$, the HEX by $HEX^{A/B/C}$, and the simple lamellar by $LAM_{\perp}^{A/B/C}$. The reason becomes clear by comparing the

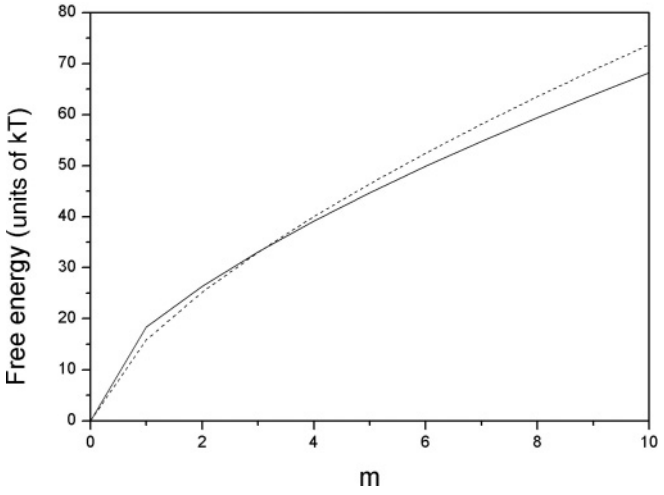

FIG. 19. Free energy of the lamellar phases as a function of the number of side chains m. Solid line represents free energy of the perpendicular lamellar-*in*-lamellar phase and the dotted line the parallel lamellar-*in*-parallel lamellar phase.

free energy of the structures considered with the free energy of simple diblocks. The difference is the extra energy due to the *C* side chains, however, this extra energy is the same for all structures considered.

When $m = 3$, the diagram is no longer similar to that of simple diblocks due to the appearance of $LAM_{||}^{A/B/C}$. Its stability region is restricted to $12 < N\chi_{AB} < 57$ for $N\chi_{AC} = N\chi_{BC} = 200$, $\phi_c = 0.7$ [Fig. 21(b)]. Increasing the AC and BC interaction to $N\chi_{AC} = N\chi_{BC} = 400$ [Fig. 21(c)] the stability region of $LAM_{||}^{A/B/C}$ also increases to $10 < N\chi_{AB} < 113$.

Finally, in Fig. 22 phase diagrams are presented in terms of the grafting density m versus the volume fraction φ_B of B blocks. For increasing m the number of segments of the repeat unit $n = 2N/m$ decreases and these diagrams are a kind of inverted versions of Fig. 20 with two differences. Due to the integer values of m we have horizontal borderlines and secondly $n\chi_{AB}$ is not fixed anymore. The most striking observation concerns the stability region of $LAM_{||}^{A/B/C}$, which strongly depends on m, the larger m, the smaller the region.

VII. CONCLUDING REMARKS

Using the strong segregation theory the self-assembly of diblock copolymer-based comb copolymers with chemically identical side chains (*A*-comb-*C*)-*b*-(*B*-comb-*C*) was investigated. Different regimes were considered. When the repulsion between the *C* side chains and the *AB* backbone is insufficient, the *C* blocks are mixed with the *AB* blocks with the *A* blocks microphase separated from the *B* blocks. In that case the behavior is equal to that of simple diblock copolymers with a renormalized Flory-Huggins parameter $(1 - \phi_C)^2\chi_{AB}$. The second case is characterized by mixed *A* and *B* blocks microphase separated from the *C* side chains. Due to the side chain architecture the phase stability region of the lamellar phase is shifted to $0.6 < \phi_C < 0.8$. For the specific case considered ($\varphi_A = \varphi_B = 0.5; m = 20$) the hexagonal structure with the core of the cylinders formed by loops from the *A* and *B*

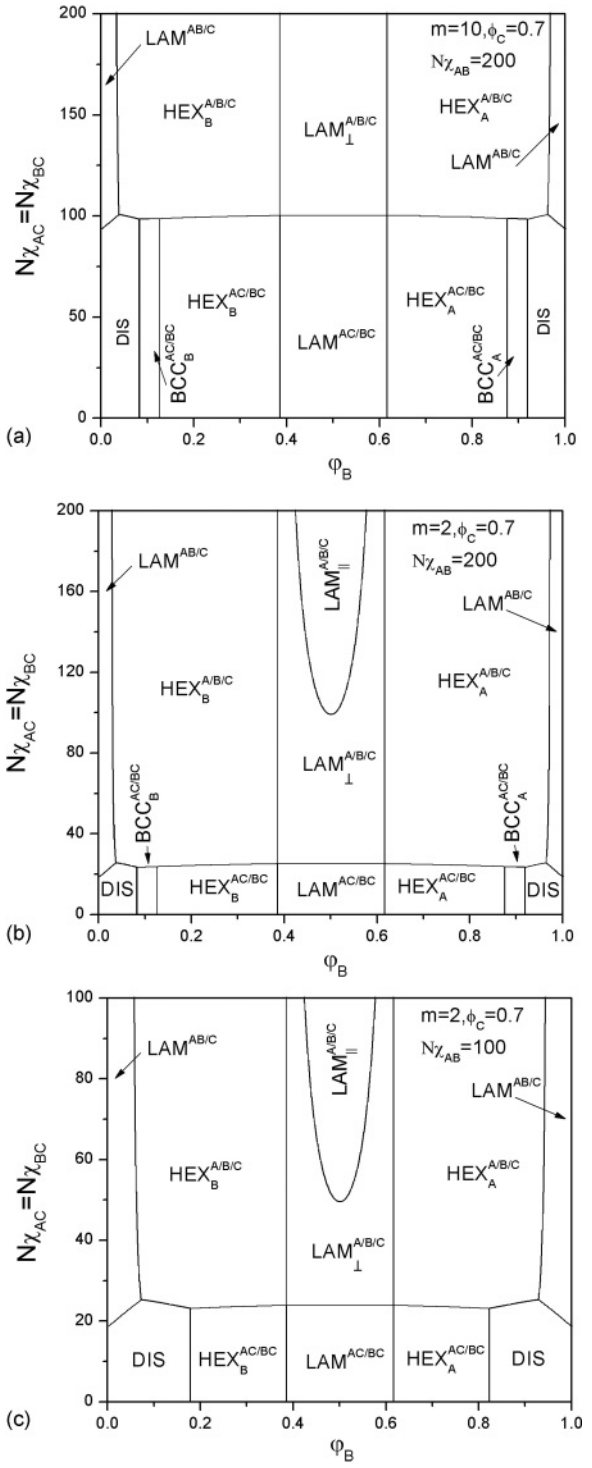

FIG. 20. Phase diagrams of (A-comb-C)-b-(B-comb-C) in terms of Flory-Huggins parameters $N\chi_{AC} = N\chi_{BC}$ vs volume fraction φ_B: (a) $m = 10, N\chi_{AB} = 200, \phi_C = 0.7$; (b) $m = 2, N\chi_{AB} = 200, \phi_C = 0.62$; and (c) $m = 2, N\chi_{AB} = 100, \phi_C = 0.7$.

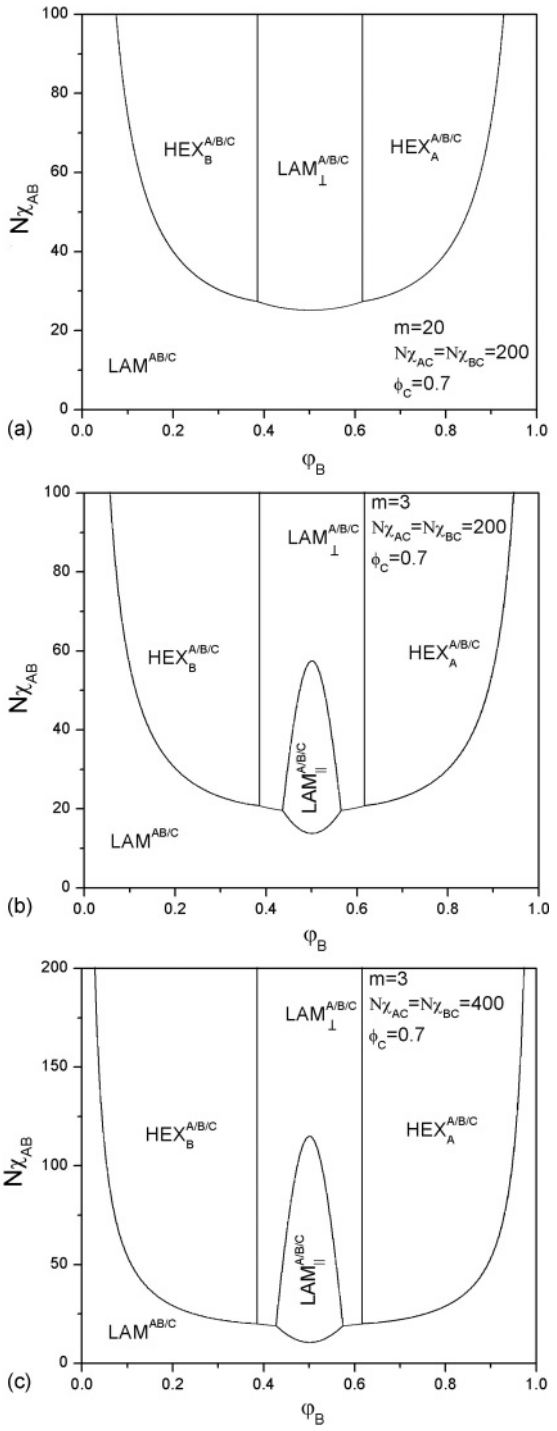

FIG. 21. Phase diagrams of (A-comb-C)-b-(B-comb-C) in terms of Flory-Huggins interaction parameter $N\chi_{AB}$ vs volume fraction φ_B: (a) $m = 10, N\chi_{AC,BC} = 200, \phi_C = 0.7$; (b) $m = 2, N\chi_{AC,BC} = 200, \phi_C = 0.7$; and (c) $m = 2, N\chi_{AC,BC} = 400, \phi_C = 0.7$.

blocks is no longer stable. Furthermore, the stability region of the bcc structure where the core of the spheres is formed by the C side chains is significantly increased compared to the simple diblock case. All these observations are in excellent agreement with previously reported results by Milner on the effect of chain architecture on the asymmetry in copolymer phase behavior [35]. The final case considered concerned the most interesting situation where all three components microphase separate from each other and hierarchically ordered structures are formed. The volume fraction of C side chains was assumed to satisfy $0.6 < \phi_C < 0.8$ so that only lamellar structures, where one layer is formed by the C side chains and the other by the

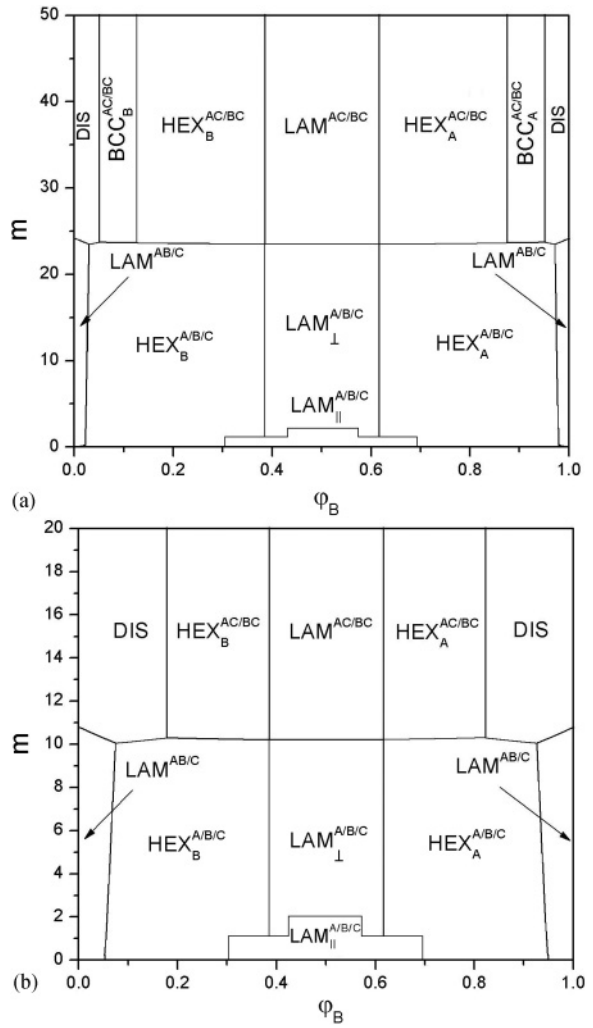

FIG. 22. Phase diagrams in terms of grafting density m vs volume fraction φ_B of B blocks: (a) $N\chi_{AB} = N\chi_{AC} = N\chi_{BC} = 200$, $\phi_C = 0.62$; and (b) $N\chi_{AB} = N\chi_{AC} = N\chi_{BC} = 100, \phi_C = 0.7$.

AB backbones, are stable. Perpendicular lamellar-*in*-lamellar and parallel lamellar-*in*-lamellar and disk-*in*-lamellar phases were found and characteristic phase diagrams presented. In the case of a lamellar-*in*-lamellar morphology, the perpendicular lamellar-*in*-lamellar is usually the preferred state. Only when the grafting density is relatively small, that is, $m \leqslant 4$, does the parallel lamellar-*in*-lamellar state become possible.

APPENDIX: CALCULATION OF THE INTERFACIAL ENERGY

The interfacial energy can be obtained from the sum of the gradient part of the conformational energy and the interaction energy,

$$\Delta F = F_{\text{grad}} + F_{\text{int}}. \tag{A1}$$

We consider two cases, namely (1) AC comb blocks microphase separated from BC comb blocks and (2) AB backbone microphase separated from C side chains. The gradient energy F_{grad} and the interaction energy F_{int} need to be calculated in each case separately.

1. *AC* comb blocks microphase separated from *BC* comb blocks

In this regime F_{grad} arises due to nonhomogeneous profiles of the A and B species, and the corresponding free energy density is given by

$$f_{\text{grad}} = \frac{a^2}{24\upsilon}\left[\frac{\phi_A'^2(z)}{\phi_A(z)} + \frac{\phi_B'^2(z)}{\phi_B(z)}\right].$$

The free energy (A1) per one copolymer chain, which occupies on average an interface area Σ, is given by

$$\begin{aligned}\Delta F_{AC/BC} = \frac{\Sigma}{\upsilon}\int_{-\infty}^{\infty} dz\Bigg\{&\frac{a^2}{24}\frac{(1-\phi_C)\,\varphi_A'^2(z)}{\varphi_A(z)\,[1-\varphi_A(z)]}\\ &+\chi_{AB}\,(1-\phi_C)^2\,\varphi_A(z)\,[1-\varphi_A(z)]\Bigg\}\\ &+\chi_{AC}\phi_C N_A + \chi_{BC}\phi_C N_B.\end{aligned} \tag{A2}$$

Here we use $\phi_j(z) = (1-\phi_C)\varphi_j(z), j = A, B$. After minimization of this expression with respect to $\varphi_A(z)$ we arrive at $\varphi_A(z) = \frac{1}{2}[1 + \tanh(\frac{z}{\Delta})]$, where $\Delta = a\sqrt{\frac{1}{6\chi_{AB}(1-\varphi_C)}}$ is the interfacial thickness. With this the free energy becomes

$$\Delta F_{AC/BC} = \Sigma\gamma_{AC/BC} + F_{AC/BC}, \tag{A3}$$

where $\gamma_{AC/BC} = \frac{a}{\upsilon}(1-\varphi_C)^{3/2}\sqrt{\frac{\chi_{AB}}{6}}$ is the effective interfacial tension and $F_{AC/BC}$ is the interaction energy of the AC/BC mixture

$$F_{AC/BC} = 2N(1-\phi_C)\phi_C(\chi_{AC}\varphi_A + \chi_{BC}\varphi_B). \tag{A4}$$

2. *AB* backbone microphase separated from *C* side chains

The free energy (A1) in this case is written as

$$\begin{aligned}\Delta F_{AB/C} = \frac{\Sigma}{\upsilon}\int_{-\infty}^{\infty} dz\Bigg\{&\frac{a^2}{24}\frac{\phi_C'^2(z)}{\phi_C(z)\,[1-\phi_C(z)]} + (\chi_{AC}\varphi_A\\ &+\chi_{BC}\varphi_B - \chi_{AB}\varphi_A\varphi_B)\phi_C(z)[1-\phi_C(z)]\Bigg\}\\ &+\chi_{AB}\varphi_A\varphi_B(N_A+N_B).\end{aligned} \tag{A5}$$

Here we used the following identity for the AB interactions:

$$\begin{aligned}\chi_{AB}\varphi_A\varphi_B[1-\phi_C(z)]^2 = {}&\chi_{AB}\varphi_A\varphi_B[1-\phi_C(z)]\\ &-\chi_{AB}\varphi_A\varphi_B\phi_C(z)[1-\phi_C(z)].\end{aligned}$$

Minimization of this free energy with respect to the concentration profile $\phi_C(z)$ gives

$$\phi_C(z) = \frac{1}{2}\left(1 + \tanh\left(\frac{z}{\Delta}\right)\right)$$

and the interfacial thickness is

$$\Delta = R_0\sqrt{\frac{1}{6(\chi_{AC}\varphi_A + \chi_{BC}\varphi_B - \chi_{AB}\varphi_A\varphi_B)}}.$$

With this the free energy becomes

$$\Delta F_{AB/C} = \Sigma\gamma_{AB/C} + \chi_{AB}\varphi_A\varphi_B(N_A+N_B). \tag{A6}$$

Here

$$\gamma_{AB/C} = \frac{a}{\upsilon}\sqrt{\frac{\chi_{AC}\varphi_A + \chi_{BC}\varphi_B - \chi_{AB}\varphi_A\varphi_B}{6}}$$

is the tension of the AB/C interface.

[1] L. Leibler, Macromolecules **13**, 1602 (1980).
[2] A. N. Semenov, Sov. Phys. JETP **61**, 733 (1985).
[3] F. S. Bates and G. H. Fredrickson, Annu. Rev. Phys. Chem. **41**, 525 (1990).
[4] M. W. Matsen and M. Schick, Phys. Rev. Lett. **72**, 2660 (1994).
[5] M. W. Matsen and F. S. Bates, Macromolecules **29**, 1091 (1996).
[6] I. W. Hamley, *The Physics of Block Copolymers* (Oxford University Press, Oxford, 1998).
[7] C. A. Tyler and D. C. Morse, Phys. Rev. Lett. **94**, 208302 (2005).
[8] M. Tanaka, T. Wakada, S. Akasaka, S. Nishitsuji, K. Saijo, H. Shimizu, M. I. Kim, and H. Hasegawa, Macromolecules **40**, 4399 (2007).
[9] F. S. Bates and G. H. Fredrickson, Phys. Today **52**, 32 (1999).
[10] V. Abetz and P. F. W. Simon, Adv. Polym. Sci. **189**, 125 (2005).
[11] C. Park, J. Yoon, and E. L. Thomas, Polymer **22**, 6725 (2003).
[12] I. W. Hamley, Angew. Chem. Int. Ed. **42**, 1692 (2003).
[13] M. Lodge, Macromol. Chem. Phys. **204**, 265 (2003).
[14] M. Lazzari, G. Liu, and S. Lecommandoux, eds., *Block Copolymers in Nanoscience* (Wiley, Weinheim, 2006).
[15] T. H. Epps III, E. W. Cochran, C. M. Hardy, T. S. Bailay, R. S. Waletzko, and F. S. Bates, Macromolecules **37**, 7085 (2004).
[16] I. Y. Erukhimovich, Eur. Phys. J. E **18**, 383 (2005).
[17] J. Masuda, A. Takano, Y. Nagata, A. Noro, and Y. Matsushita, Phys. Rev. Lett. **97**, 098301 (2006).
[18] Y. Smirnova, G. ten Brinke, and I. Y. Erukhimovich, J. Chem. Phys. **124**, 054907 (2006).
[19] Y. Matsushita, Macromolecules **40**, 771 (2007).
[20] K. Hayashida, T. Dotera, A. Takano, and Y. Matsushita, Phys. Rev. Lett. **98**, 195502 (2007).
[21] Z. Guo, G. Zhang, F. Qiu, H. Zhang, Y. Yang, and A-C. Shi, Phys. Rev. Lett. **101**, 028301 (2008).
[22] M. Sun, P. Wang, F. Qiu, P. Tang, H. Zhang, and Y. Yang, Phys. Rev. E **77**, 016701 (2008).
[23] J. Qin, F. S. Bates, and D. C. Morse, Macromolecules **43**, 5128 (2010).
[24] G. Zhang, F. Qiu, H. Zhang, Y. Yang, and A-C. Shi, Macromolecules **43**, 2981 (2010).
[25] M. Olvera de la Cruz and I. C. Sanchez, Macromolecules **19**, 2501 (1986).
[26] H. Benoit and G. Hadziioannou, Macromolecules **21**, 1449 (1988).
[27] A. V. Dobrynin and I. Y. Erukhimovich, Macromolecules **26**, 276 (1993).
[28] A. Shinozaki, D. Jasnow, and A. C. Balazs, Macromolecules **27**, 2496 (1994).
[29] D. P. Föster, D. Jasnow, and A. C. Balazs, Macromolecules **28**, 3450 (1995).
[30] L. Wang, L. Zhang, and J. Lin, J. Chem. Phys. **129**, 114905 (2008).
[31] C. Lee, S. P. Gido, Y. Poulos, N. Hadjichristidis, N. B. Tan, S. F. Trevino, and J. W. Mays, J. Chem. Phys. **107**, 6460 (1997).
[32] C. Lee, S. P. Gido, Y. Poulos, N. Hadjichristidis, N. B. Tan, S. F. Trevino, and J. W. Mays, Polymer **39**, 4631 (1988).
[33] M. Xenidou, F. L. Beyer, N. Hadjichristidis, S. P. Gido, and N. B. Tan, Macromolecules **31**, 7659 (1998).
[34] F. L. Beyer *et al*., Macromolecules **33**, 2039 (2000).
[35] S. T. Milner, Macromolecules **27**, 2333 (1994).
[36] R. J. Nap, C. Kok, G. ten Brinke, and S. I. Kuchanov, European Phys. J. E **4**, 515 (2001).
[37] R. J. Nap and G. ten Brinke, Macromolecules **35**, 952 (2002).
[38] J. Ruokolainen, R. Mäkinen, M. Torkkeli, T. Mäkelä, R. Serimaa, G. ten Brinke, and O. Ikkala, Science **280**, 557 (1998).
[39] J. Ruokolainen, G. ten Brinke, and O. Ikkala, Adv. Mater. **11**, 777 (1999).
[40] O. Ikkala and G. ten Brinke, Science **295**, 2407 (2002).
[41] H.-L. Chen, J.-S. Liu, C.-H. Yu, C.-L. Yeh, U.-S. Jeng, and W.-C. Chen, Macromolecules **40**, 3271 (2007).
[42] W.-S. Chiang, C.-H. Lin, B. Nandan, C.-L. Yeh, M. H. Rahman, W.-C. Chen, and H.-L. Chen, Macromolecules **41**, 8138 (2008).
[43] A. H. Hofman, V. Voet, G. ten Brinke, and K. U. Loos (unpublished).